Subcritical Crack Propagation and Coalescence Induced by the Oil-Gas Transformation

Zhi-Qiang Fan[1], Zhi-He Jin[1*] , Scott. E. Johnson[2]

[1]Department of Mechanical Engineering, University of Maine, Orono, ME 04469, USA
[2]School of Earth and Climate Sciences, University of Maine, Orono, ME 04469, USA
* Corresponding author: zhihe.jin@maine.edu

Abstract The present work develops a multi-physics model to investigate subcritical propagation of initially oil-filled, sub-horizontal collinear microcracks driven by the excess pressure induced during the conversion of oil to gas in a petroleum source rock under continuous burial. The crack propagation distance, propagation duration, crack coalescence and overpressure in the crack are determined using a finite difference scheme that couples linear elastic fracture mechanics, oil-gas transformation kinetics and an equation of state for the gas. The numerical results for a source rock with typical properties show that when the crack spacing is greater than $b/a_0 = 3$ (where a_0 is the half crack length and b the half distance between crack centers) the cracks do not coalesce and the duration of gas-driven crack propagation is governed by the transformation kinetics because the subcritical crack propagation rate is much faster than the oil-gas conversion rate. The collinear cracks coalesce for smaller crack spacing and the crack propagation duration may be reduced significantly due to crack interactions. The multi-physics model developed in this work together with our previous model for crack propagation during conversion of solid kerogen to oil indicates that microcracks resulting from buildup of excess fluid pressure during hydrocarbon generation may serve as an effective pathway for primary petroleum migration.

Keywords: Collinear cracks, Migration, Oil-gas conversion, Overpressure, Subcritical growth

1. Introduction

Overpressures widely observed in the deep part of sedimentary basins coincident with primary zones of gas generation are commonly attributed to thermal cracking of kerogen to oil/gas and oil to gas. Microfractures are a common feature of petroleum source rocks in these basins interpreted to serve as migration conduits for oil and gas [1]. Understanding the dominant mechanisms responsible for the microfracture initiation and development in petroleum source rocks at great depth is crucial for hydrocarbon exploration and safe drilling.

Fine grained source rocks like shales rich in kerogen undergo progressive burial, which leads to an increase in bulk density and loss of porosity. With increasing depth of burial, there is also a marked decrease in permeability. As temperatures and pressures increases, kerogen breaks down to release oil when it becomes mature. Conversion of kerogen to oil results in significant volume increase due to the density difference between the precursors and the products. Meanwhile, part of the overburden load will be transferred to the newly generated oil. As a natural result, overpressure is generated [2, 3]. Clay-sized minerals within source rocks functioning as effective seals enable local overpressure build-up [1]. When the overpressure exceeds the mechanical strength of the source rocks, microfractures around kerogen particles are initiated, thus creating a migration pathway for oil [4, 5].

As burial proceeds, temperatures continue to increase. When the gas window is reached, oil retained in the microfractures will be subjected to thermal cracking to form gas, which consists predominantly of methane [2-3]. The volume increase associated with transformation of oil to gas is more appreciable. According to Barker [6], less than two percent of oil conversion to gas would

readily create overpressure in excess of lithostatic pressure and cause microfracturing in an effectively sealed reservoir. As a result, microfractures driven by the overpressure may grow and coalesce to form interconnected fracture networks, which may facilitate further migration of hydrocarbons [2, 7].

Convincing evidence from field observations has been presented to support the concept that microfractures induced by overpressure from hydrocarbon generation serve as migration conduits for hydrocarbons. Examples include the Bakken shale in Williston Basin [8], La Luna source rocks in the Maracaibo Basin [9], Woodford Formation in Oklahoma and Arkansas [10], fractured source rocks from the Oligocene Frio Formation, Texas [11], mature shales in the Hils area in Germany [12] and Alberta Basin in Canada [13]. Detailed observations by Lash and Engelder [14] showed that layer parallel microcracks filled with bitumen in organic-rich Dunkirk shale of Catskill delta, New York resulted from hydrocarbon generation. Common features of these microfractures in overpressured source rocks are summarized as follows: (1) the microcracks are of opening mode, i.e. mode I; (2) the preferred orientation of microfractures is parallel or sub-parallel to bedding plane; (3) most microcracks contain bitumen or calcite, showing the characteristic of petroleum generation; and (4) microfractures are found in organic-rich source rocks at high maturity level.

More recently, Jin et al. [4] developed a model of primary migration of oil by collinear microcrack coalescing during the main stage of oil generation and found that microfractures propagate subcritically since excess pressure resulted from kerogen conversion to oil is not high enough to drive critical crack growth. In the present paper we extend our previous work to investigate subcritical growth of a series of periodically spaced subhorizontal collinear microfractures driven by excess fluid pressure due to thermal cracking of oil to gas. As a special case, the propagation of a single crack is also studied. We focus on the effects of gas compressibility and crack spacing on the crack propagation behavior including crack propagation distance and duration, as well as excess pressure evolution.

2. Formulation of theoretical model of crack propagation during gas generation

2.1. Thermal cracking of oil to gas

Transformation of oil to gas satisfies the following first order differential equation [15]

$$\frac{dM}{dt} = -BM \exp\left[-\frac{E_A}{RT(t)}\right] \tag{1}$$

where M is the mass of convertible oil at time t, B is a pre-exponential constant, E_A is the activation energy of the transformation, R is the universal gas constant, and T is the absolute temperature. We assume a constant burial rate S and a constant geothermal gradient G so that the depth of burial z and time-varying temperature T can be written as

$$z(t) = H_0 + St\,, \quad T(t) = T_0 + G(z - H_0) = T_0 + GSt \tag{2}$$

where H_0 is the initial burial depth at which the oil-filled cracks are located, T_0 is the corresponding temperature at H_0. By integrating Eq. (1) with Eq. (2) and using mass conservation, Fan et al. [7] obtained the volumes of oil and gas at time t as follows

$$V_{oil}^t = M_0 \exp\left[-\Phi(t)\right]/\rho_{oil}\,, \quad V_{gas}^t = M_0\left\{1 - \exp\left[-\Phi(t)\right]\right\}/\rho_{gas} \tag{3}$$

where M_0 is the initial mass of oil, ρ_{oil} is the density of oil, ρ_{gas} is the gas density which is a function of pressure and temperature determined by the equation of state (EOS), and $\Phi(t)$ is given by

$$\Phi(t)=\frac{B(T_0+GSt)}{GS}\exp\left[-\frac{E_A}{R(T_0+GSt)}\right]-\frac{BT_0}{GS}\exp\left(-\frac{E_A}{RT_0}\right)+\frac{BE_A}{RGS}\left[E_i\left(-\frac{E_A}{R(T_0+GSt)}\right)-E_i\left(-\frac{E_A}{RT_0}\right)\right] \tag{4}$$

in which $E_i(\ )$ is the exponential integral defined by

$$E_i(x)=\int_{-\infty}^{x}\frac{e^{x'}}{x'}dx' \tag{5}$$

2.2. An equation of state (EOS) for gas

To account for the compressibility of gas under subsurface conditions, we adopt an EOS for methane developed by Duan et al. [16], since natural gas consists primarily of methane. The EOS, which is capable to describe the behavior of methane with high accuracy over wide temperature and pressure range (0 - 1000 ^{o}C and 0 - 800 MPa, respectively), takes the form

$$\frac{P_rV_r}{T_r}=1+\frac{C_1}{V_r}+\frac{C_2}{V_r^2}+\frac{C_3}{V_r^4}+\frac{C_4}{V_r^5}+\frac{C_5}{V_r^2}\left(\beta+\frac{\gamma}{V_r^2}\right)\exp\left(-\frac{\gamma}{V_r^2}\right) \tag{6}$$

where $P_r=P/P_c$, $T_r=T/T_c$, $V_r=V/V_c$, P and T are the pressure and temperature of the gas, respectively, $V = m/\rho_{\text{gas}}$ is the molar volume with m denoting the molar mass, T_c is the critical temperature above which methane can not be liquefied regardless of the pressure applied, P_c is the critical pressure required to liquefy methane at the critical temperature T_c, $V_c = RT_c/P_c$, and

$$C_1=a_1+\frac{a_2}{T_r^2}+\frac{a_3}{T_r^3}\quad C_2=a_4+\frac{a_5}{T_r^2}+\frac{a_6}{T_r^3},\ C_3=a_7+\frac{a_8}{T_r^2}+\frac{a_9}{T_r^3},\ C_4=a_{10}+\frac{a_{11}}{T_r^2}+\frac{a_{12}}{T_r^3},\ C_5=\frac{\alpha}{T_r^3} \tag{7}$$

The EOS contains 15 material constants: a_i (i = 1, 2… 12), α, β and γ， which can be found in [16].

From Eq. (6) we can express gas pressure in terms of gas density and temperature as follows

$$P=P(\rho_{gas})=\frac{P_cT_rV_c\rho_{gas}}{m}\left[1+\frac{BV_c\rho_{gas}}{m}+\frac{CV_c^2\rho_{gas}^2}{m^2}+\frac{DV_c^4\rho_{gas}^4}{m^4}+\frac{EV_c^5\rho_{gas}^5}{m^5}+\frac{FV_c^2\rho_{gas}^2}{m^2}\left(\beta+\frac{\gamma V_c^2\rho_{gas}^2}{m^2}\right)\exp\left(-\frac{\gamma V_c^2\rho_{gas}^2}{m^2}\right)\right] \tag{8}$$

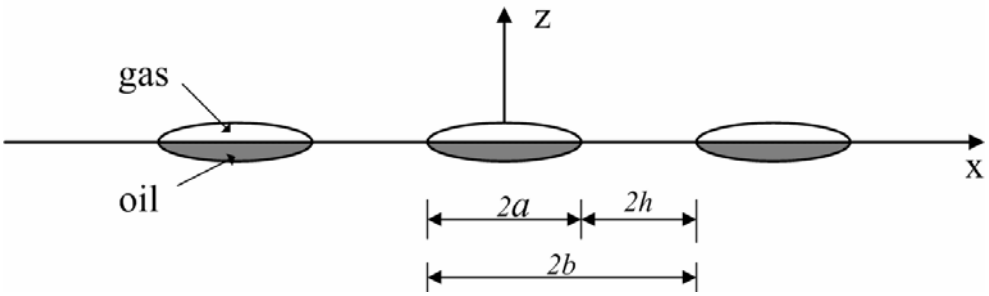

Figure 1. Subhorizontal periodically spaced collinear microcracks filled by oil and gas

2.3. Fracture mechanics model

Consider a row of periodic collinear microcracks initially filled by oil within a source rock under continuous burial as shown in Figure 1, where $2a = 2a\ (t)$ denotes the crack length at time t and

$2h$ is the crack spacing. Initially the crack is subjected to uniform oil pressure on the crack surface. The initial excess pressure is denoted by Δp_0 which is the oil pressure beyond the overburden pressure. The excess pressure increases as oil to gas conversion proceeds. At time t, the excess pressure can be obtained as follows

$$\Delta p = P(\rho_{gas}) - \rho_s g z = P(\rho_{gas}) - \rho_s g\left(H_0 + St\right) \tag{9}$$

where ρ_s is the average sediment density, g = 9.8 m/s^2 is gravitational acceleration, and $P(\rho_{gas})$ is the gas pressure given by Eq. (8).

The stress intensity factor (SIF) at the crack tips is given by

$$K_I = \Delta p\sqrt{2b\tan\left(\frac{\pi a}{2b}\right)} \tag{10}$$

where $b = a + h$. The volume per unit thickness in the y direction of the crack is

$$V_{crack}^{t} = \frac{16b^2\Delta p\left(1-\nu^2\right)}{\pi E}\ln\left[\sec\left(\frac{\pi a}{2b}\right)\right] \tag{11}$$

where E and ν are Young's modulus and Poisson's ratio of the source rock, respectively. Since the crack is fully saturated with oil and gas, the volume of the crack must equal the sum of oil and gas volumes, that is,

$$V_{oil}^{t} + V_{gas}^{t} = V_{crack}^{t} \tag{12}$$

From Eq. (11), we can get the initial mass of oil within the crack

$$M_0 = \frac{16b^2\rho_{oil}\Delta p_0\left(1-\nu^2\right)}{\pi E}\ln\left[\sec\left(\frac{\pi a_0}{2b}\right)\right] \tag{13}$$

where a_0 is the half initial crack length. Clearly the SIF increases with the increasing excess pressure.

Subcritical crack propagation will be initiated once the SIF reaches a threshold value K_{Ith}, but less than the rock fracture toughness K_{Ic}. Generally, the subcritical crack growth can be described by the Charles power law [17]

$$v = \frac{da}{dt} = A\left[K_I(a)\right]^n \tag{14}$$

where ν is the subcritical propagation velocity, n is the subcritical crack growth index and A is a material constant. It follows from Eq. (10) that the excess fluid pressure corresponding to the onset of subcritical crack growth is

$$\Delta p_{th} = K_{\mathrm{I}th} / \sqrt{2b\tan\left(\frac{\pi a_0}{2b}\right)} \tag{15}$$

The corresponding crack volume is

$$V_{crack}^{0} = \frac{16b^2\left(1-\nu^2\right)K_{\mathrm{I}th}}{\pi E\sqrt{2b\tan\left(\frac{\pi a_0}{2b}\right)}}\ln\left[\sec\left(\frac{\pi a_0}{2b}\right)\right] \tag{16}$$

The time needed for the excess pressure to reach Δp_{th} from the start of oil-gas transformation, denoted by t_0, can be determined by solving the following two equations

$$P\left(\rho_{gas}^{th}\right) - \rho_s g(H_0 + St_0) = K_{\mathrm{I}th} / \sqrt{2b\tan\left(\frac{\pi a_0}{2b}\right)} \tag{17}$$

$$\frac{M_0\left\{1-\exp\left[-\Phi\left(t_0\right)\right]\right\}}{\rho_{gas}^{th}}+\frac{M_0\exp\left[-\Phi\left(t_0\right)\right]}{\rho_{oil}}=\frac{16b^2\left(1-\nu^2\right)\Delta p_{th}}{\pi E}\ln\left[\sec\left(\frac{\pi a_0}{2b}\right)\right] \tag{18}$$

where ρ_{gas}^{th} is the corresponding gas density at time t_0.

2.4. Simulation of subcritical crack propagation and coalescence using finite difference

A finite difference formulation is used to study the coupling between gas generation from oil degradation and gas expulsion through microfracture propagation and coalescence. Consider the microcrack propagation from time t_0 to current time t. We subdivide the time domain into N intervals to construct a mesh of equally-spaced grids: $t_0, t_1,\ldots, t_{N-1}, t_N$ with $t_N=t$. The following notations are adopted. $a_i=a(t_i)$ and $\rho_{gas}^i=\rho_{gas}(t_i)$ represent the half crack length and the corresponding gas density at time step t_i , respectively. Replace the derivative in Eq. (14) by a forward difference approximation at time t_i, then we obtain the following expression for the half crack length at t_{i+1}

$$a_{i+1}=a_i+A[P(\rho_{gas}^i)-\rho_s g\left(H_0+St_i\right)]^n(2b)^{n/2}\left[\tan\left(\frac{\pi a_i}{2b}\right)\right]^{n/2}(t_{i+1}-t_i) \tag{19}$$

Neglecting the mutual solubility of gas and oil, we obtain the oil and gas volumes at t_{i+1} as follows

$$V_{oil}^{i+1}=\frac{M_0\exp\left[-\Phi\left(t_{i+1}\right)\right]}{\rho_{oil}},\qquad V_{gas}^{i+1}=\frac{M_0\left\{1-\exp\left[-\Phi\left(t_{i+1}\right)\right]\right\}}{\rho_{gas}^{i+1}} \tag{20}$$

where ρ_{gas}^{i+1} is the gas density at time step t_{i+1}. The volume of the crack at t_{i+1} is by Eq. (11) applied at step t_{i+1}.

The requirement that crack volume must be equal to the sum of oil and gas volumes yields the excess pressure Δp_{i+1} at t_{i+1},

$$\Delta p_{i+1}=M_0\left[\frac{\exp\left[-\Phi\left(t_{i+1}\right)\right]}{\rho_{oil}}+\frac{\left\{1-\exp\left[-\Phi\left(t_{i+1}\right)\right]\right\}}{\rho_{gas}^{i+1}}\right]\Bigg/\left\{\frac{16b^2\left(1-\nu^2\right)}{\pi E}\ln\left[\sec\left(\frac{\pi a_{i+1}}{2b}\right)\right]\right\} \tag{21}$$

Note that $\Delta p_{i+1}=P(\rho_{gas}^{i+1})-\rho_s g\left(H_0+St_{i+1}\right)$, and then we can solve this equation for the unknown gas density ρ_{gas}^{i+1}. Consequently the excess pressure Δp_{i+1} at t_{i+1} can be obtained using Eq. (21). To drive the crack growth subcritically, Δp_{i+1} must satisfy the following condition

$$\Delta p_{i+1}\geq K_{1th}/\sqrt{2b\tan\left(\frac{\pi a_{i+1}}{2b}\right)} \tag{22}$$

Otherwise, we need to adjust time t_{i+1} by solving Eq. (17) and (18) with a_0, t_0 and ρ_{gas}^{th} replaced by a_{i+1}, t_{i+1} and ρ_{gas}^{i+1}, respectively.

3. Numerical Results and Discussions

This section presents numerical examples to illustrate effects of initial burial depth and crack spacing on the excess pressure evolution with time and crack propagation distance for a single crack, and propagation and coalescence of collinear cracks. Since shales are major source rocks for oil and natural gas, in our simulation we study shales for illustration purpose. Typically thermal cracking of oil is initiated at temperatures of 120-160 ^oC, and ultimate conversion to methane may occur at

temperatures in excess of 200 ^{o}C, at depth of burial ranging between 3000m and 7000m [19]. We examine the sensitivity of crack propagation to variations of initial depth of burial in the range of 3500-5000m. The initial temperature is assumed as T_0 = 150 ^{o}C. We also assume that $\Delta p_0 = \Delta p_{th}$ and the stress intensity factor equals the threshold value K_{Ith} due to the excess oil pressure at the initial state. Other physical and geometrical parameters used in our simulation are summarized in Table 1[14, 16-19].

Table 1 Physical and geometrical parameters used in the numerical simulation

Symbols	Definition	Value(unit)
Rock Matrix		
E	Young's modulus	2.0 GPa
ν	Poison's ratio	0.4
ρ_s	Average sediment density	2350 kg/m^3
K_{Ith}	Threshold stress intensity factor	0.06 MPa-m$^{1/2}$
A	Subcritical crack growth constant	10^7 m/s/(MPa-m$^{1/2}$)^{10}
n	Subcritical crack growth index	10
a_0	Initial half crack length	50 μm
H_0	Initial depth of burial	4000 m
T_0	Initial temperature	150 ^{o}C
G	Geothermal gradient	30 ^{o}C/km
S	Burial rate	0.1 km/M.y.
Oil		
ρ_{oil}	Oil density	850 kg/m^3
Methane		
m	Molar mass	16 g/mol
T_c	Critical temperature	191.1 K
P_c	Critical pressure	4.64 MPa
Kinetics		
B	Pre-exponential constant	1.744×10^{13} sec^{-1}
E_A	Activation energy	217.6 kJ/mol
R	Universal gas constant	8.314 J/mole/K

3.1 Single crack case

When $b/a_0 \rightarrow \infty$ the crack interaction disappears and the problem reduces to the single crack case. Figures 2 shows crack propagation distance versus time corresponding to three different values of H_0 for a single crack. The corresponding excess pressure profiles are shown in Figure 3. Similar to the kerogen conversion to oil case [4], subcritical crack propagation rate is much faster than the oil-gas conversion rate, so the crack propagation duration is governed by the oil-gas transformation kinetics. The excess pressure decreases monotonically as crack propagation distance increases with time, which is indicated by Eq. (10). It is seen from Figure 2 that the final crack length increases with decreasing initial depth of burial. It can be explained by considering the gas compressibility in Eq. (8). Gas density increases monotonically with increasing depth of burial, so the density difference between the transformation precursor and end product becomes smaller. Therefore, the crack propagation distance becomes smaller at greater depth of burial. From Figure 3 we can see that at a given time, the excess pressure within the crack is lower at a shallower depth of burial because longer cracks require smaller overpressure to grow as suggested by Eq. (10).

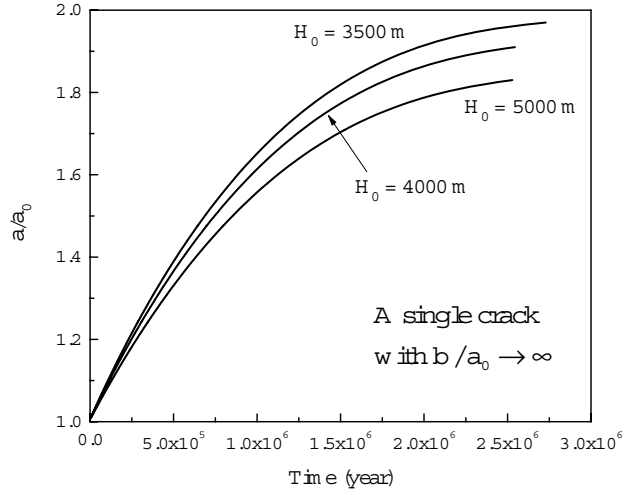

Figure 2. Crack propagation distance versus time for a single crack corresponding to different initial depths of burial

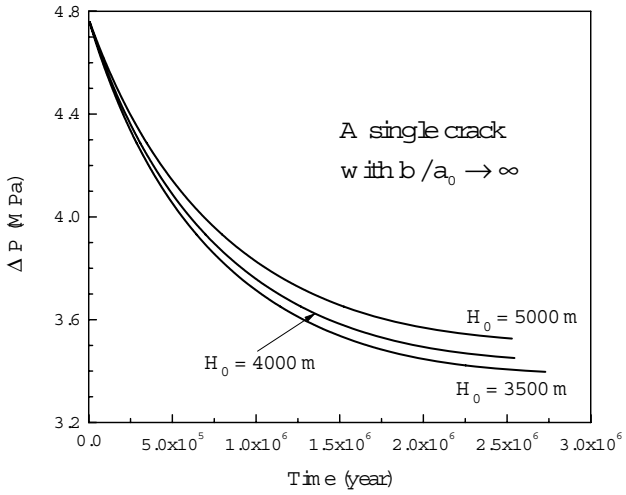

Figure 3. Excess pressure evolution over time for a single crack corresponding to different initial depths of burial

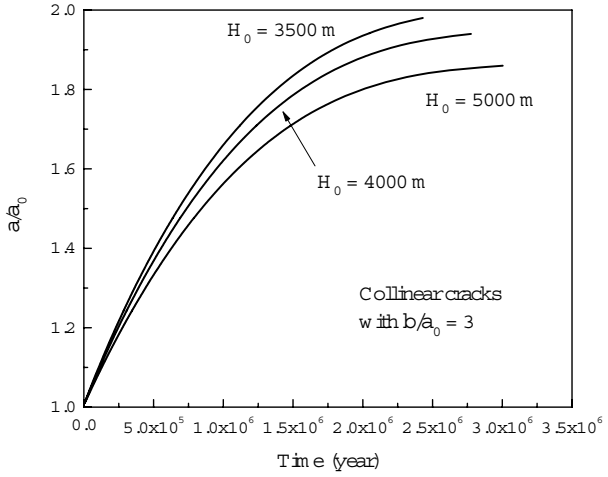

Figure 4. Effect of initial depth of burial on the crack propagation distance for collinear cracks with initial crack spacing $b/a_0 = 3$

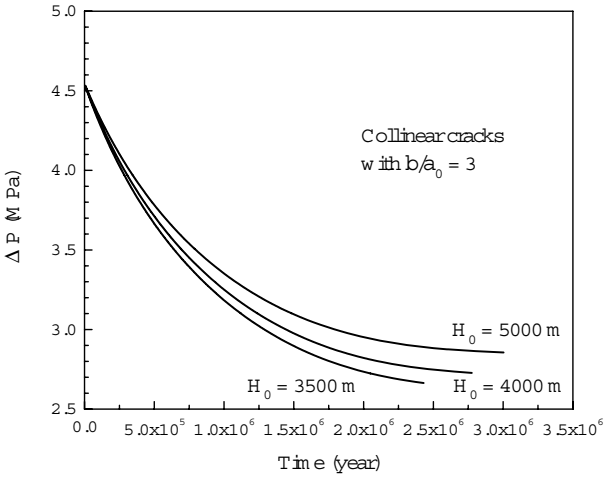

Figure 5. Effect of initial depth of burial on the excess pressure for collinear cracks with initial crack spacing $b/a_0 = 3$

3.2 Collinear cracks case

The effects of initial burial depth on crack propagation distance and excess pressure evolution for b/a_0=3 are shown in Figures 4 and 5, respectively. The general trends in the variation of crack propagation distance and excess pressure with time corresponding to different H_0 are quite similar to those observed in Figures 2 and 3, respectively. A particularly noteworthy feature is sharp differences on the crack propagation duration between a single crack and collinear cracks at shallow burial depth. For example, Figure 2 shows that it takes about 2.74 million years for the single crack to grow to 1.97 times its original length when all the oil within the crack converts to gas completely. For collinear cracks, it takes about 2.42 million years to grow to 1.98 times its original length and the microcracks are almost to coalesces (b/a_0=3 and h/a_0=2) to form macroscopic cracks. The

marked decrease in crack propagation duration is due to rapid acceleration of crack growth associated with drastic increase in stress intensity factor as crack spacing decreases.

We also examine the sensitivity of crack propagation distance and excess pressure to the changes of crack spacing, as shown in Figures 6 and 7, respectively. Our numerical calculation shows that when $b/a_0 > 3$, no crack coalescence is found for typical burial depth in the range of 3000-7000m where thermal cracking of oil to gas occurs. For $b/a_0 = 2.0$, the excess pressure decreases with time and drops sharply when the cracks are about to coalesce. Due to crack interaction, the threshold excess pressure to initiate subcritical crack growth increases with increasing crack spacing. The crack propagation reduces significantly for smaller crack spacing. For example, the crack propagation duration is about 3.39 million years for $b/a_0=5$. It reduces to about 1.09 million years when $b/a_0=2$.

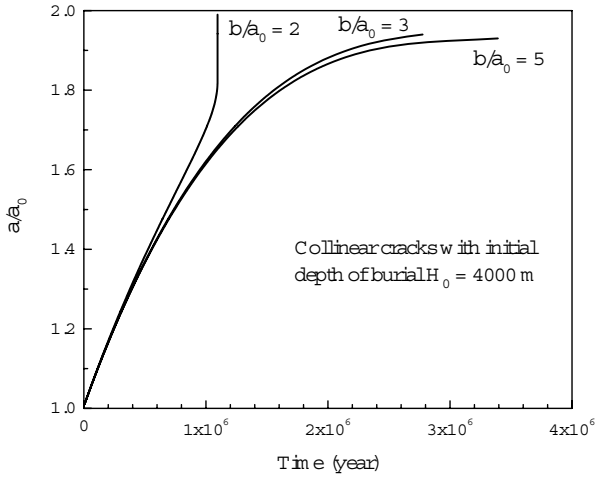

Figure 6. Effect of crack spacing on the crack propagation distance for collinear cracks with initial depth of burial $H_0 = 4000$ m

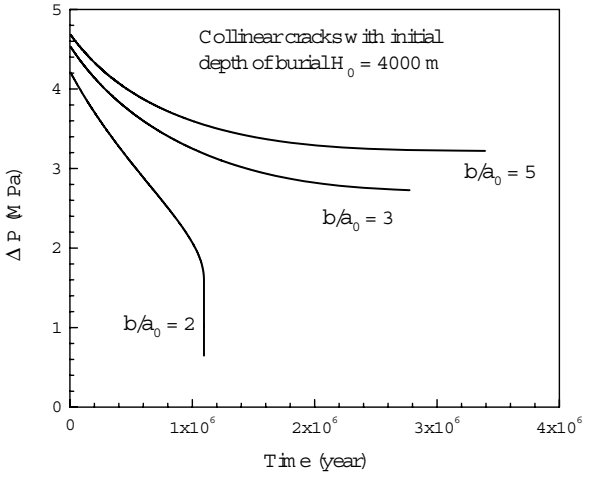

Figure 7. Effect of crack spacing on the crack propagation distance for collinear cracks with initial depth of burial $H_0 = 4000$ m

Concluding Remarks

To address the coupling between gas generation and expulsion, we develop a theoretical model to study the gas migration through propagation and coalescence of collinear microfractures initially filled by oil incorporating fracture mechanics of source rocks, geochemistry of thermal cracking of oil to gas, and an equation of state for gas. Based on our numerical simulation, the following conclusions can be reached, which may provide some insight into gas migration process.

(1) Gas expulsion through self-propagating microfractures is an effective mechanism for primary migration within well-sealed source rocks and excess pressure caused by thermal cracking of oil to gas serves as driving force for microfracture propagation.

(2) Increasing depth of burial leads to decreasing crack propagation distance due to gas compressibility. Therefore cracks at shallower depth are more likely to form interconnected fracture network.

(3) Crack spacing has a significant effect on crack propagation duration for collinear cracks with smaller crack spacing leading to shorter crack propagation duration.

References

[1] Momper, J. A., Oil migration limitations suggested by geological and geochemical considerations, *AAPG Course Note Series*, 8**(**1978), B1–B60.
[2] Hunt, J. M., *Petroleum geochemistry and geology*, Freeman, San Francisco, 1979.
[3] Tissot, B.P. & Welte D.H., Petroleum formation and occurrence, *A New Approach to Oil and Gas Exploration*, Springer, Berlin, 1984.
[4] Jin, Z.-H., Johnson, S.E. & Fan, Z.Q., Subcritical propagation and coalescence of oil-filled cracks: getting the oil out of low-permeability source rocks, *Geophys. Res. Lett.*, 37 (2010), L01305.
[5] Fan, Z. Q., Jin, Z.-H. & Johnson, S. E., Subcritical propagation of an oil-filled penny-shaped crack during kerogen–oil conversion, *Geophys. J. Int.*, 182 (2010), 1141–1147.
[6] Barker, C, Calculated volume and pressure changes during the thermal-cracking of oil to gas in reservoirs. AAPG Bull, 74(1990): 1254-1261.
[7] Fan, Z. Q., Jin, Z.-H. & Johnson, S. E., Gas-driven subcritical crack propagation during the conversion of oil to gas, *Petrol. Geosci.*, 18(2012): 191-199.
[8] Meissner, F. F., Petroleum geology of the bakken formation williston basin, north Dakota and Montana. Williston Basin Symposium, Montana Geological Society, 24th Annual Conference, 1978
[9] Talukdar, S., Observations on the primary migration of oil in the la luna source rocks of the maracaibo basin, venezuela. in. Doligez B., (Ed). Migration of hydrocarbons in sedimentary basins, Editions Technip. Paris, 1987, pp59-77
[10] Comer, J.B. & Hinch, H.H., Recognizing and quantifying expulsion of oil from the Woodford Formation and age-equivalent rocks in Oklahoma and Arkansas, *AAPG Bull.*, 71 (1987) 844–858.
[11] Capuano, R.M., Evidence of fluid flow in microcracks in geopressured shales, *AAPG Bull.*, 77 (1993), 1303–1314.
[12] Littke, R., D. R. Baker and D. Leythaeuser , Microscopic and sedimentologic evidence for the generation and migration of hydrocarbons in toarcian source rocks of different maturities. Org. Geochem., 13(1988), 549-559.
[13] Marquez, X.M. & Mountjoy, E.W., Microcracks due to overpressure caused by thermal cracking in well-sealed Upper Devonian reservoirs, deep Alberta basin, *AAPG Bull.*, 80 (1996), 570–588.
[14] Lash, G.G. & Engelder, T., An analysis of horizontal microcracking during catagenesis: an example from the Catskill delta complex, *AAPG Bull.*, 89 (2005), 1433–1449.
[15] Berg, R.R. & Gangi, A.F., Primary migration by oil-generation microfracturing in low-permeability source rocks: application to the Austin Chalk, Texas, *AAPG Bull.*, 83 (1999), 727–756.
[16] Duan, Z. H., Moller, N. & Weare, J. N., An equation of state for the CH_4-CO_2-H_20 system: I. Pure systems from 0 to 1000^{o}C and 0 to 8000 bar, *Geochim. Cosmochim. Acta*, 56 **(**1992), 2605-2617.
[17] Atkinson, B.K., Subcritical crack growth in geological materials, *J. geophys. Res.*, **89**(1984), 4077–4144.
[18] Pepper A. S. & Corvi P. J., Simple kinetic models of petroleum formation. Part I: oil and gas generation from kerogen, *Mar. Petrol. Geol.*, 12 (1995), 291–319.
[19] Schmidt, R. Fracture mechanics of oil shale-unconfined fracture toughness, stress corrosion cracking, and tension test results. The 18th US Symposium on Rock Mechanics (USRMS), Golden, Colorada, Colorado School of Mines, 1977.